

New Production Mechanism for Heavy Neutrinos at the LHC

P. S. Bhupal Dev,¹ Apostolos Pilaftsis,^{1,2} and Un-ki Yang³

¹*Consortium for Fundamental Physics, School of Physics and Astronomy,
University of Manchester, Manchester, M13 9PL, United Kingdom*

²*CERN, Department of Physics, Theory Division, CH-1211 Geneva 23, Switzerland*

³*Department of Physics and Astronomy, Seoul National University, Seoul 151-747, Korea*

(Dated: January 10, 2014)

We study a new production mechanism for heavy neutrinos at the LHC, which dominates over the usually considered s -channel W -exchange diagram for heavy-neutrino masses larger than 100–200 GeV. The new mechanism is infrared-enhanced by t -channel $W\gamma$ -fusion processes. This has important implications for experimental tests of the seesaw mechanism of neutrino masses, and in particular, for the ongoing heavy neutrino searches at the LHC. We find that the direct collider limits on the light-to-heavy neutrino mixing can be significantly improved, when this new production channel is properly taken into account. The scope of this new mechanism can equally well be extended to other exotic searches at the LHC.

The discovery of nonzero neutrino masses and mixing from neutrino oscillation data provides the first (and so far only) conclusive experimental evidence of the existence of new physics beyond the Standard Model (SM). A simple paradigm for understanding the smallness of neutrino masses in a natural way is the seesaw mechanism [1]. Its simplest realization [2] (known as the type-I seesaw) requires the existence of a set of heavy SM-singlet Majorana fermions N , which break the $(B - L)$ -symmetry of the theory by two units. The seesaw scale is synonymous with the typical Majorana mass M_N of these heavy neutrinos, whose origin must be connected with some new physics [1]. In the flavor basis $\{(\nu_L)^C, N\}$, the seesaw mass matrix has the following general structure [2, 3]:

$$\mathcal{M}_\nu = \begin{pmatrix} 0 & M_D \\ M_D^\top & M_N \end{pmatrix}, \quad (1)$$

where M_D is the Dirac mass term which mixes the light (ν_L) and heavy (N) states. In the usual seesaw approximation: $\|\xi\| \ll 1$, where $\xi \equiv M_D M_N^{-1}$ and $\|\xi\| \equiv \sqrt{\text{Tr}(\xi^\dagger \xi)}$, this leads to the observed light neutrino mass matrix of the form

$$M_\nu \simeq -M_D M_N^{-1} M_D^\top \quad (2)$$

and to the light-to-heavy neutrino mixing of order ξ [3]. We note that the smallness of M_ν could be attributed to a very high value for M_N , or to a particular flavor structure in (2), or both. Without specifying the details of the model, we generically call this minimal realization the ‘SM seesaw’.

As mentioned above, there are two key aspects of the seesaw mechanism that can be probed experimentally: the Majorana mass M_N of the heavy neutrinos, and the mixing ξ between the heavy and light neutrinos. The Majorana nature of the light and heavy neutrinos can in principle be tested via neutrinoless double beta decay ($0\nu\beta\beta$) [4]. However, this does not necessarily probe the mixing ξ whose effects may be sub-dominant, compared to purely left-(or right-)handed contributions to the $0\nu\beta\beta$

process. Alternatively, a non-negligible value for ξ could be inferred from non-unitarity of the light neutrino mixing matrix [5], in neutrino oscillation data, as well as in observables for lepton flavor violation (LFV) [6]. However, these low-energy observables by themselves do not prove the Majorana nature of heavy neutrinos since models with pseudo-Dirac heavy neutrinos can also yield large non-unitarity and LFV effects [7].

In the SM seesaw, the Majorana nature of possible electroweak-scale heavy neutrinos as well as their mixing with the light neutrinos can be *simultaneously* unraveled via their distinctive like-sign dilepton signatures at colliders [8]. The usually considered production channel for heavy Majorana neutrinos at the LHC is $pp \rightarrow W^\pm \rightarrow \ell^\pm N$ (Fig. 1), with N subsequently decaying to $\ell^\pm W$, followed by the W -decay to hadronic final states. For $M_N > M_W$, the W -boson produced from the pp collision is off-shell, whereas that coming from the N -decay is on-shell. For a Majorana neutrino N , this leads to the ‘smoking-gun’ collider signature of same-sign dileptons plus two jets with no missing energy ($\ell^\pm \ell^\pm jj$). This was first pointed out in the context of Left-Right models [9], and was subsequently analyzed in [10–13] within the SM seesaw. Experimental searches based on this channel have been performed using the $\sqrt{s} = 7$ TeV LHC data for the di-muon case [14, 15] (and also for the di-electron case [15]). No excess above the expected SM background has been observed so far, and upper limits on the light-to-heavy neutrino mixing parameter squared, $|V_{\mu N}|^2 \approx (\xi \xi^\dagger)_{\mu\mu} = 10^{-2} - 10^{-1}$, have been derived for heavy neutrino masses $M_N = 100 - 300$ GeV.

For collider tests of the SM seesaw to be effective, the mixing parameter $V_{\ell N} \approx \xi_{\ell N}$ must be significant, since this is the only way the heavy neutrino communicates to the observable SM sector. This requires that apart from M_N being small (in the sub-TeV to TeV range to be kinematically accessible), M_D must be large (in the few GeV range) simultaneously. In the traditional “vanilla” seesaw mechanism, we expect the light-to-heavy neutrino

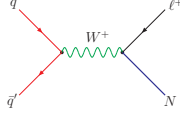


FIG. 1. The usually considered heavy neutrino production channel in the SM seesaw at the LHC.

mixing $V_{\ell N} \sim \sqrt{m_\nu/M_N} \lesssim 10^{-7}$ for $M_N \sim 1$ TeV, due to the smallness of light neutrino mass $m_\nu \lesssim 0.1$ eV [16], thus making the collider signal unobservable. However, if the Dirac and Majorana mass matrices in (2) have specific textures which can be enforced by some symmetries [10, 17], $V_{\ell N}$ can be naturally large while the light neutrinos remain massless at the tree-level. The observed non-zero neutrino masses and mixing can be generated by approximately breaking the underlying symmetry structure via radiative effects and/or higher-dimensional operators. Such models allow the possibility of having $\mathcal{O}(100)$ GeV heavy Majorana neutrinos with a significant $V_{\ell N}$, and hence, observable lepton number violation (LNV) at the LHC [18], without being in conflict with the neutrino oscillation data. We will generically assume this for our subsequent discussion, without referring to any particular texture or model-building aspects, and so treat M_N and $V_{\ell N}$ as free phenomenological parameters.

In this Letter we explicitly demonstrate the existence of a novel production mechanism for heavy neutrinos at the LHC which dominates over the previously considered s -channel W -exchange diagram shown in Fig. 1. Within the SM seesaw, there exist many reactions at parton level listed in [11], which give rise to same-sign dileptons with $n \geq 2$ jets. The contributions of most of these additional diagrams are negligible compared to the that in Fig. 1, and have therefore been neglected in all previous collider analyses. As we show below, however, diagrams involving virtual photons in the t -channel as shown in Fig. 2 give rise to *diffraction* processes, such as

$$pp \rightarrow W^* \gamma^* jj \rightarrow \ell^\pm N jj, \quad (3)$$

which are *not* negligible, but infrared enhanced. In fact, the inclusive cross section of these processes is divergent due to the collinear singularity caused by the photon propagator. As we increase the virtuality of the photon by giving a large transverse momentum to the associated jet (p_T^j), the cross section becomes finite. Following the Weizsäcker-Williams equivalent photon approximation (EPA) for electrons [19], we may analogously write down the cross section as a convolution of the probability that the proton radiates off a real photon, by absorbing the collinear divergence of the low- p_T regime into an effective photon structure function for the proton [20, 21].

To establish the importance of the diagrams in Fig. 2, we compare the inclusive cross section for $N\ell^\pm jj$ with

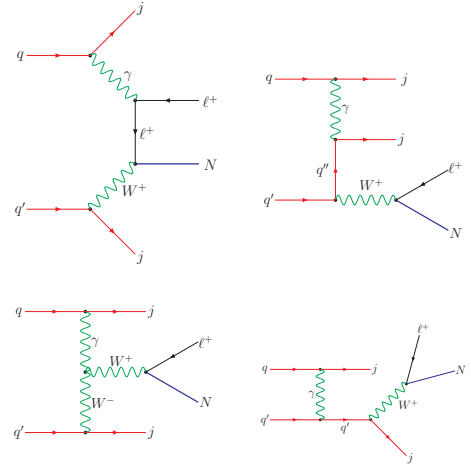


FIG. 2. New heavy neutrino production channels at the LHC. Mirror-symmetric and Z -mediated graphs are not shown.

the previously considered $N\ell^\pm$ in Fig. 1. Note that the $pp \rightarrow N\ell^\pm jj$ process receives contributions from both hadronic and electroweak processes. The hadronic channels mediated by virtual gluons and quarks give $\mathcal{O}(\alpha_s)$ corrections to the production channel in Fig. 1 and drop at the same rate as the $pp \rightarrow N\ell^\pm$ cross section, as the heavy neutrino mass increases. The electroweak contributions come from the virtual γ -exchange diagrams shown in Fig. 2, and also from additional $W^\pm Z$ -mediated graphs not shown here. All these Feynman graphs must be taken into account, in order to get a gauge-invariant result. It turns out that the total electroweak contribution drops at a rate slower than the $pp \rightarrow N\ell^\pm$ cross section with increasing heavy neutrino mass. This is mainly due to the infrared-enhanced cross section of the γ -mediated processes in 3, which have a significantly milder dependence on M_N . As a result, the production channel (3) dominates over the earlier considered $pp \rightarrow N\ell^\pm$ channel with increasing M_N . Similar behavior is also expected with increasing center of mass energy \sqrt{s} in the pp collisions, as verified by our numerical simulations given below. Thus, the process (3) becomes increasingly important for heavy neutrino searches at the LHC, for higher energies \sqrt{s} and also larger M_N values. Consequently, it must be taken into account in present and future analyses of the LHC data.

Our numerical results are shown in Fig. 3 for the inclusive production cross sections normalized to the mixing parameter $|V_{\ell N}|^2 = 1$. For the process $pp \rightarrow N\ell^\pm jj$, we obtain the ‘inclusive’ cross section by applying a minimal jet p_T cut of $p_T^j > (p_T^j)_{\min}$ to avoid the collinear singularity, whereas the infrared part is approximated by the inclusive cross section of the process $p\gamma \rightarrow N\ell^\pm j$, where the photon comes from a proton. The latter process was calculated with EPA using the improved

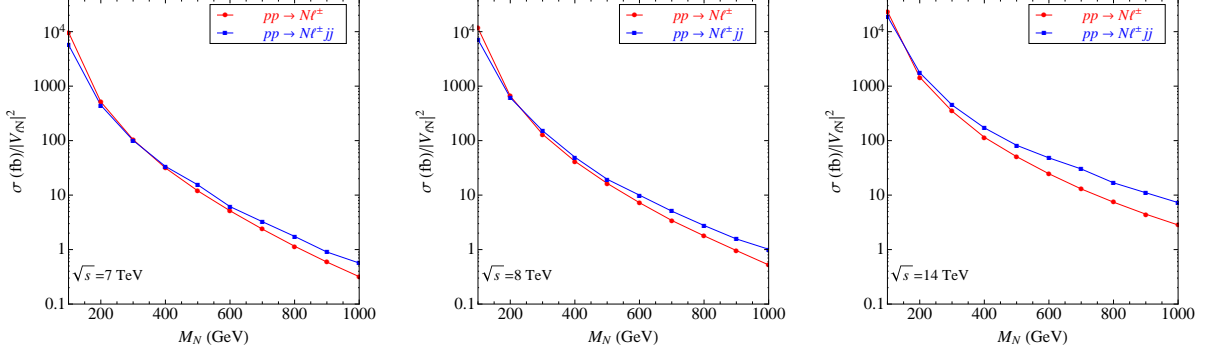


FIG. 3. Comparison of the inclusive cross sections for the heavy neutrino production channels $pp \rightarrow N\ell^\pm$ and $pp \rightarrow N\ell^\pm jj$ at LHC energies of $\sqrt{s} = 7, 8$ and 14 TeV.

Weizsäcker-Williams formula [20] for a fixed factorization scale of $\mu_F = (p_T^j)_{\min}$. For concreteness, we have chosen $(p_T^j)_{\min} = 10$ GeV (the lowest detection threshold for ATLAS) and used the equivalent photon distribution functions as implemented in **MadGraph5** [22], whereas the quark and gluon distribution functions of the proton were taken from **CTEQ6L** [23]. The renormalization scale was chosen for each event depending on the maximum final-state mass (M_N in our case). Note that the total cross section which is a sum of the $pp \rightarrow N\ell^\pm jj$ and $p\gamma \rightarrow N\ell^\pm j$ cross sections should be independent of the p_T^j cut, as long as the collinear part of the $pp \rightarrow N\ell^\pm jj$ process is consistently absorbed into the photon distribution function. We observed some discrepancy from this general expectation, which could be due to the fact that the accuracy of EPA, while being excellent for elastic scattering processes [24], is scale-dependent for inelastic channels [25], and moreover, the choice of the factorization scale is not unique due to higher order effects in perturbative QCD. For an alternative model of EPA as currently implemented in **CalcHEP3.4** [26], we get similar results as above for the $p\gamma \rightarrow N\ell^\pm j$ cross sections within 10-20% accuracy. However, since the dominant contribution results from the process $pp \rightarrow N\ell^\pm jj$ in the current mass range of interest, this point will not affect the main results of the analysis presented here.

From Fig. 3 we see that the $N\ell^\pm$ production channel is dominant only in the low mass regime, whilst the new $N\ell^\pm jj$ channel starts becoming dominant for $M_N \gtrsim 300$ GeV at $\sqrt{s} = 7$ TeV LHC. This crossover point shifts towards lower values of M_N , with increasing \sqrt{s} . It is interesting to note that the existing heavy neutrino searches [14, 15] have only explored up to $M_N = 300$ GeV with $\sqrt{s} = 7$ TeV LHC data, but plan to extend up to $M_N = 500$ GeV with $\sqrt{s} = 8$ TeV data. Hence, the new production channel proposed here must be taken into account in *all* current and future LHC analyses.

An important consequence of the new production

mechanism for heavy neutrinos is that the current LHC sensitivity for the light-to-heavy neutrino mixing parameter $V_{\mu N}$ can be improved significantly for the whole heavy neutrino mass range of interest, i.e. $M_N = 100 - 300$ GeV. In order to derive the new limits on $V_{\mu N}$, we first calculate the efficiency of the new signal proposed here: $pp \rightarrow N\mu^\pm jj \rightarrow \mu^\pm \mu^\pm 4j$, after implementing the same selection criteria as used for the $\mu^\pm \mu^\pm jj$ channel in the $\sqrt{s} = 7$ TeV ATLAS analysis [14]:

$$\begin{aligned} p_T^j &> 20 \text{ GeV}, \quad p_T^\mu > 20 \text{ GeV}, \quad p_T^{\mu, \text{leading}} > 25 \text{ GeV}, \\ |\eta^j| &< 2.8, \quad |\eta^\mu| < 2.5, \quad \Delta R^{jj} > 0.4, \quad \Delta R^{\mu j} > 0.4, \\ m_{\mu\mu} &> 15 \text{ GeV}, \quad E_T^{\text{miss}} < 35 \text{ GeV}, \quad m_{jj} \in [55, 120] \text{ GeV}, \end{aligned} \quad (4)$$

and for $\Delta R^{\mu j} < 0.4$, we require $p_T^\mu > 80$ GeV to retain muons close to jets from event topologies with boosted heavy neutrinos. After generating the parton level events with **MadGraph5** [22], the showering and hadronization were performed with **Pythia6.4** [27] and a fast detector simulation was done using **DELPHES2.0.5** [28]. Jets are reconstructed using the anti- k_T jet clustering algorithm with $R = 0.4$ as implemented in **FastJet2** [29]. We find that the total selection efficiency for the $\mu^\pm \mu^\pm$ signal remains almost the same as before [14], since the additional two jets coming from the new channel are usually lost due to the stringent selection criteria given in (4). Regarding the SM background for these processes, we expect the background for di-muon+ n jets (with $n \geq 2$) to be the same as that reported in [14] for the selection criteria in (4). Note that the SM backgrounds for the $\mu^\pm \mu^\pm 4j$ signal reported here mainly come from $t\bar{t}+V$ (where $V = W, Z$) and WW production, which are small compared to the WZ background for the $\mu^\pm \mu^\pm jj$ signal [14]. A separate dedicated set of selection criteria and background reduction methods must be designed in order to distinguish the new $\mu^\pm \mu^\pm 4j$ signal from the usual $\mu^\pm \mu^\pm jj$ signal, and this will be studied elsewhere. A similar analysis can also be performed for the di-electron signal $e^\pm e^\pm nj$

(with $n \geq 2$). Although the limits on $|V_{eN}|^2$ derived from $0\nu\beta\beta$ constraints are much more stringent [8], models with quasi-degenerate heavy Majorana neutrinos may naturally evade these constraints, while giving rise to sizeable LNV signals at the LHC [13]. For the corresponding limits on $|V_{\tau N}|^2$, the identification of same-sign di-tau events at the LHC is quite difficult, thus making a realistic collider simulation for this case rather involved.

Following a rather conservative approach to our analysis here, we use the current 95% confidence level upper limits on the cross section $\sigma(pp \rightarrow \mu^\pm \mu^\pm jj)$ [14], derived from the $\sqrt{s} = 7$ TeV LHC data with 4.7 fb^{-1} luminosity, and translate them into upper limits on the mixing parameter $|V_{\mu N}|^2$ as shown in Fig. 4 by dividing the cross section limits by the total inclusive cross section $\sigma(pp \rightarrow \mu^\pm \mu^\pm nj)$ (with $n \geq 2$). We find that the existing ATLAS limits [14] are improved by almost 50% with the inclusion of the new production mechanism. For comparison, we also show the corresponding CMS limits [15] which are much weaker compared to those by ATLAS, mainly due to their large backgrounds. The horizontal line shows the current best limit on $|V_{\mu N}|^2$ derived indirectly from electroweak precision data [30] which is independent of the heavy neutrino mass for $M_N > M_Z$. Note that the LFV processes (such as rare lepton decays [31] and $\mu - e$ conversion [32]) put stringent constraints on the product $|V_{\ell N} V_{\ell' N}^*|$ (with $\ell \neq \ell'$) [6], thereby limiting the LHC sensitivity for LFV signals of the type $e^\pm \mu^\pm jj$; however, they do not restrict the individual mixing parameters $|V_{\ell N}|^2$. In order to compare the direct search limits with the indirect one, we also derive our expected upper limits for $\sqrt{s} = 8$ and 14 TeV LHC by assuming that the corresponding experimental upper limits on the signal cross section will be *at least* as good as the $\sqrt{s} = 7$ TeV results. Again, these are conservative limits as the experimental limits on cross section are expected to improve significantly with the analysis of more data, if no signal is observed. In that case, the direct collider limits could surpass the indirect limits for a significant range of heavy neutrino masses, once the new production mechanism proposed here is considered. In particular, Fig. 4 shows that the effect of the new production mechanism at LHC energies $\sqrt{s} = 14$ TeV will be to improve the current ATLAS limit by *at least* a factor of five.

In summary, we have analyzed a new dominant production mechanism for heavy neutrinos at the LHC. This mechanism is extremely important for the range of heavy neutrino masses currently being searched for and provides significantly improved *direct* limits on the light-to-heavy neutrino mixing $V_{\ell N}$, in a fully independent fashion of the indirect searches. As more data are gathered at the LHC and the sensitivity to higher heavy neutrino mass ranges is contemplated, these new contributions will be crucial in setting the best possible direct limits on the mixing parameter $V_{\mu N}$ in the absence of a signal. On the other hand, an evidence of LNV at the LHC could

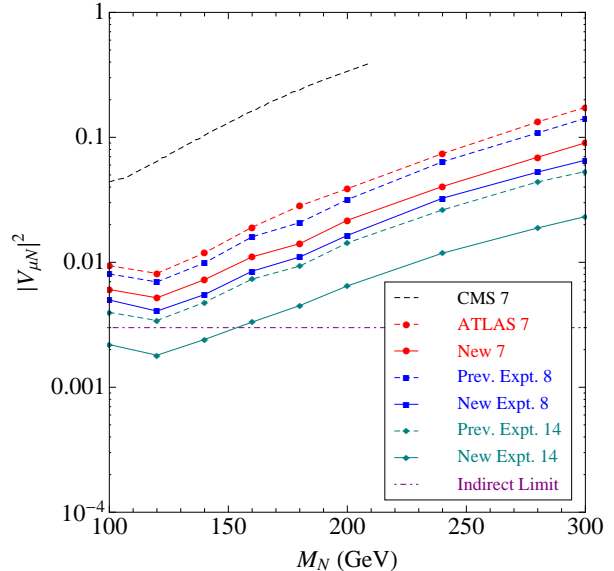


FIG. 4. Improved upper limits (solid lines, also labeled “New”) on the mixing parameter $|V_{\mu N}|^2$ for LHC energies $\sqrt{s} = 7, 8$ and 14 TeV, along with the current CMS [15] and ATLAS [14] limits derived at $\sqrt{s} = 7$ TeV, and the conservative upper limits expected for 8- and 14-TeV LHC runs using the *previous* production mode of Fig. 1 (dashed lines, also labeled “Prev.”). The horizontal line shows the current best limit on $|V_{\mu N}|^2$ from indirect searches [30].

reveal underlying symmetries of the lepton sector, thus shedding light on the seesaw mechanism. We should note that the scope of the new infrared-enhanced production mechanism proposed here is not just limited to heavy Majorana neutrinos, and can also be applied to other heavy particle searches (the so-called ‘exotics’) at the LHC. For instance, for pseudo-Dirac heavy neutrinos, the same production channels studied here could give rise to an enhanced tri-lepton signal. This mechanism is also applicable for searches of vector-like fermions and new charged scalars. We hope to address some of these aspects in a future communication.

P.S.B.D. and A.P. thank Mike Seymour for helpful discussions on the equivalent photon approximation. P.S.B.D. also thanks Francisco del Aguila and Rabindra Mohapatra for useful discussions on lepton number violation, Olivier Mattelaer for help with photon structure functions in **MadGraph**, John Almond and Joel Klinger for clarifications on the ATLAS selection cuts used here. The work of P.S.B.D. and A.P. is supported by the Lancaster-Manchester-Sheffield Consortium for Fundamental Physics under STFC grant ST/J000418/1. In addition, A.P. gratefully acknowledges partial support by a IPPP associateship from Durham University.

-
- [1] For a review, see R. N. Mohapatra and A. Y. Smirnov, *Ann. Rev. Nucl. Part. Sci.* **56**, 569 (2006) [hep-ph/0603118].
- [2] P. Minkowski, *Phys. Lett. B* **67**, 421 (1977); R. N. Mohapatra and G. Senjanović, *Phys. Rev. Lett.* **44**, 912 (1980); T. Yanagida, *Workshop on unified theories and baryon number in the universe*, eds. A. Sawada and A. Sugamoto, KEK, Tsukuba (1979); M. Gell-Mann, P. Ramond and R. Slansky, *Supergravity*, ed. P. Van Nieuwenhuizen and D. Freeman, North Holland, Amsterdam (1980).
- [3] J. Schechter and J. W. F. Valle, *Phys. Rev. D* **22**, 2227 (1980); *Phys. Rev. D* **25**, 774 (1982).
- [4] For reviews, see e.g., W. Rodejohann, *Int. J. Mod. Phys. E* **20**, 1833 (2011) [arXiv:1106.1334 [hep-ph]]; F. F. Depisch, M. Hirsch and H. Pas, *J. Phys. G* **39**, 124007 (2012) [arXiv:1208.0727 [hep-ph]].
- [5] S. Antusch, C. Biggio, E. Fernandez-Martinez, M. B. Gavela and J. Lopez-Pavon, *JHEP* **0610**, 084 (2006) [hep-ph/0607020]; A. Abada, C. Biggio, F. Bonnet, M. B. Gavela and T. Hambye, *JHEP* **0712**, 061 (2007) [arXiv:0707.4058 [hep-ph]].
- [6] For a review, see M. Raidal *et al.*, *Eur. Phys. J. C* **57**, 13 (2008) [arXiv:0801.1826 [hep-ph]].
- [7] M. Malinsky, T. Ohlsson and H. Zhang, *Phys. Rev. D* **79**, 073009 (2009) [arXiv:0903.1961 [hep-ph]]; M. Malinsky, T. Ohlsson, Z.-z. Xing and H. Zhang, *Phys. Lett. B* **679**, 242 (2009) [arXiv:0905.2889 [hep-ph]]; P. S. B. Dev and R. N. Mohapatra, *Phys. Rev. D* **81**, 013001 (2010) [arXiv:0910.3924 [hep-ph]]; D. V. Forero, S. Morisi, M. Tortola and J. W. F. Valle, *JHEP* **1109**, 142 (2011) [arXiv:1107.6009 [hep-ph]].
- [8] For a review, see A. Atre, T. Han, S. Pascoli and B. Zhang, *JHEP* **0905**, 030 (2009) [arXiv:0901.3589 [hep-ph]].
- [9] W.-Y. Keung and G. Senjanović, *Phys. Rev. Lett.* **50**, 1427 (1983).
- [10] A. Pilaftsis, *Z. Phys. C* **55**, 275 (1992) [hep-ph/9901206].
- [11] A. Datta, M. Guchait and A. Pilaftsis, *Phys. Rev. D* **50**, 3195 (1994) [hep-ph/9311257].
- [12] F. M. L. Almeida, Jr., Y. D. A. Coutinho, J. A. Martins Simoes and M. A. B. do Vale, *Phys. Rev. D* **62**, 075004 (2000) [hep-ph/0002024]; O. Panella, M. Cannoni, C. Carimalo and Y. N. Srivastava, *Phys. Rev. D* **65**, 035005 (2002) [hep-ph/0107308]; T. Han and B. Zhang, *Phys. Rev. Lett.* **97**, 171804 (2006); F. del Aguila, J. A. Aguilar-Saavedra and R. Pittau, *JHEP* **0710**, 047 (2007) [hep-ph/0703261]; F. del Aguila and J. A. Aguilar-Saavedra, *Nucl. Phys. B* **813**, 22 (2009) [arXiv:0808.2468 [hep-ph]].
- [13] S. Bray, J. S. Lee and A. Pilaftsis, *Nucl. Phys. B* **786**, 95 (2007) [hep-ph/0702294].
- [14] ATLAS Collaboration, ATLAS-CONF-2012-139.
- [15] S. Chatrchyan *et al.* [CMS Collaboration], *Phys. Lett. B* **717**, 109 (2012) [arXiv:1207.6079 [hep-ph]].
- [16] P. A. R. Ade *et al.* [Planck Collaboration], arXiv:1303.5076 [astro-ph.CO].
- [17] J. Gluza, *Acta Phys. Polon. B* **33**, 1735 (2002) [hep-ph/0201002]; A. Pilaftsis, *Phys. Rev. Lett.* **95**, 081602 (2005) [hep-ph/0408103]; J. Kersten and A. Y. Smirnov, *Phys. Rev. D* **76**, 073005 (2007) [arXiv:0705.3221 [hep-ph]]; Z.-z. Xing, *Prog. Theor. Phys. Suppl.* **180**, 112 (2009) [arXiv:0905.3903 [hep-ph]]; X.-G. He, S. Oh, J. Tandean and C.-C. Wen, *Phys. Rev. D* **80**, 073012 (2009) [arXiv:0907.1607 [hep-ph]]; A. Ibarra, E. Molinaro and S. T. Petcov, *JHEP* **1009**, 108 (2010) [arXiv:1007.2378 [hep-ph]]; F. F. Depisch and A. Pilaftsis, *Phys. Rev. D* **83**, 076007 (2011) [arXiv:1012.1834 [hep-ph]]; P. S. B. Dev, C.-H. Lee and R. N. Mohapatra, *Phys. Rev. D* **88**, 093010 (2013) [arXiv:1309.0774 [hep-ph]].
- [18] Even for quasi-degenerate heavy Majorana neutrinos (as occurs in specific models), the LNV signal can be sizable when the mass splitting $\Delta M_N \equiv M_{N_1} - M_{N_2}$ is comparable to the width $\Gamma_N \equiv (\Gamma_{N_1} + \Gamma_{N_2})/2$ [13]. For instance, for the on-shell production of $N_{1,2}$ with average four-momentum squared $\bar{s} = (M_{N_1}^2 + M_{N_2}^2)/2$, the LNV amplitude in the muon-channel is given by $\mathcal{A}_{\text{LNV}}^{\mu\mu}(\bar{s}) = -V_{\mu N_1}^2 \frac{2\Delta M_N}{\Delta M_N^2 + \Gamma_N^2} + \mathcal{O}\left(\frac{\Delta M_N}{M_{N_1}}\right)$, for $\Delta M_N \lesssim \Gamma_N$.
- [19] C. F. von Weizsäcker, *Z. Phys.* **88**, 612 (1934); E. J. Williams, *Phys. Rev.* **45**, 729 (1934).
- [20] V. M. Budnev, I. F. Ginzburg, G. V. Meledin and V. G. Serbo, *Phys. Rept.* **15**, 181 (1974).
- [21] S. Frixione, M. L. Mangano, P. Nason and G. Ridolfi, *Phys. Lett. B* **319**, 339 (1993) [hep-ph/9310350]; M. Glück, C. Pisano and E. Reya, *Phys. Lett. B* **540**, 75 (2002) [hep-ph/0206126].
- [22] J. Alwall, M. Herquet, F. Maltoni, O. Mattelaer and T. Stelzer, *JHEP* **1106**, 128 (2011) [arXiv:1106.0522 [hep-ph]].
- [23] J. Pumplin, D. R. Stump, J. Huston, H. L. Lai, P. M. Nadolsky and W. K. Tung, *JHEP* **0207**, 012 (2002) [hep-ph/0201195].
- [24] B. A. Kniehl, *Phys. Lett. B* **254**, 267 (1991).
- [25] C. Pisano, *Eur. Phys. J. C* **38**, 79 (2004).
- [26] A. Belyaev, N. D. Christensen and A. Pukhov, *Comput. Phys. Commun.* **184**, 1729 (2013) [arXiv:1207.6082 [hep-ph]].
- [27] T. Sjostrand, S. Mrenna and P. Z. Skands, *JHEP* **0605**, 026 (2006) [hep-ph/0603175].
- [28] S. Ovin, X. Roubey and V. Lemaitre, arXiv:0903.2225 [hep-ph]; J. de Favereau *et al.*, arXiv:1307.6346 [hep-ex].
- [29] M. Cacciari, G. P. Salam and G. Soyez, *Eur. Phys. J. C* **72**, 1896 (2012) [arXiv:1111.6097 [hep-ph]].
- [30] F. del Aguila, J. de Blas and M. Perez-Victoria, *Phys. Rev. D* **78**, 013010 (2008) [arXiv:0803.4008 [hep-ph]].
- [31] A. Ilakovac and A. Pilaftsis, *Nucl. Phys. B* **437**, 491 (1995) [hep-ph/9403398].
- [32] R. Alonso, M. Dhen, M. B. Gavela and T. Hambye, *JHEP* **1301**, 118 (2013) [arXiv:1209.2679 [hep-ph]].